

Suspension System Modeling and Simulation

Walden Marshall

November 2021

1 Introduction

In the United States and worldwide, automobiles are the most common mode of transportation. We depend on our cars to be fast, reliable, safe and comfortable. Our safety and comfort depend on, among other things, the design of our cars' suspension systems. In this work, we examine simplified models of suspension systems and, through simulation, observe their performance as the car drives over a pothole.

2 Quarter-Car Model

2.1 Linear Damping

For most basic engineering applications, suspension systems are modeled as a mass-spring-damper, a second order linear system. This model relies on the following assumptions:

- A. The only forces acting on the mass (vehicle) are gravity, an external forcing function, and the forces from the spring and damper.¹
- B. The spring obeys Hooke's Law, $F_s = -kz$, where z is the displacement from the spring's equilibrium, F_s is the restorative force exerted by the spring, and k is known as the spring constant.
- C. The damper exerts a force on the mass antiparallel and proportional to the mass' velocity. This can be expressed as $F_d = -c\dot{z}$, where F_d is the force from the damper, c is the damping coefficient and \dot{z} is the velocity, the time derivative of position.

A free body diagram for a generic mass-spring-dashpot system is shown in **Figure 1**. Using Newton's Second Law, $\Sigma F = ma$, we can fairly easily derive a differential equation of motion for the system:

¹While Assumption A includes gravity in the model, we need not actually include gravity in any calculations. This is because the force due to gravity will cause the spring to compress to some equilibrium position. By simply letting $z = 0$ at this position, we remove any need to include a $F_g = mg$ term.

$$\begin{aligned}
 m\ddot{z} &= ma = \Sigma F = F_{ext} + F_d + F_s \\
 &= F_{ext} - c\dot{z} - kz
 \end{aligned}$$

Moving all terms with z dependence to the left side, we can see that the equation of motion is a second order, nonhomogenous, linear differential equation with constant coefficients.

$$m\ddot{z} + c\dot{z} + kz = F_{ext}(t) \quad (1)$$

Equation 1 can be modeled with the Simulink block diagram shown in **Figure 2**.

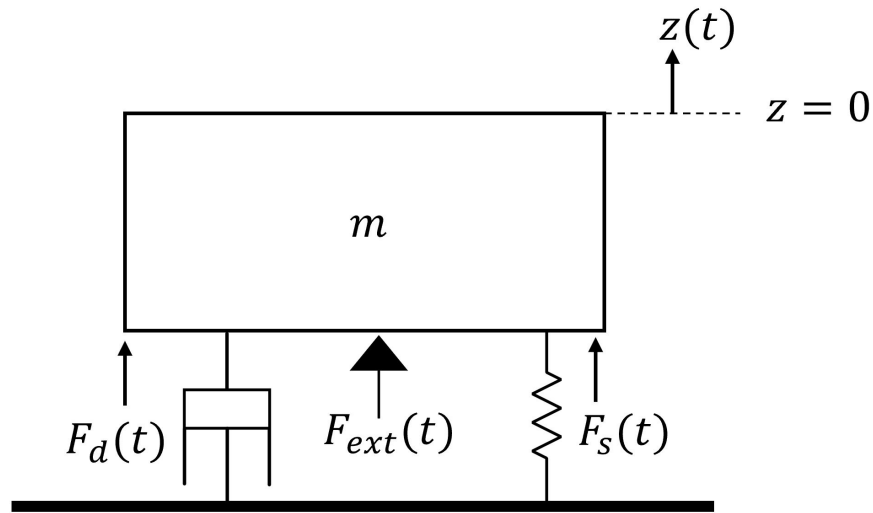


Figure 1: Free body diagram for mass-spring-dashpot system

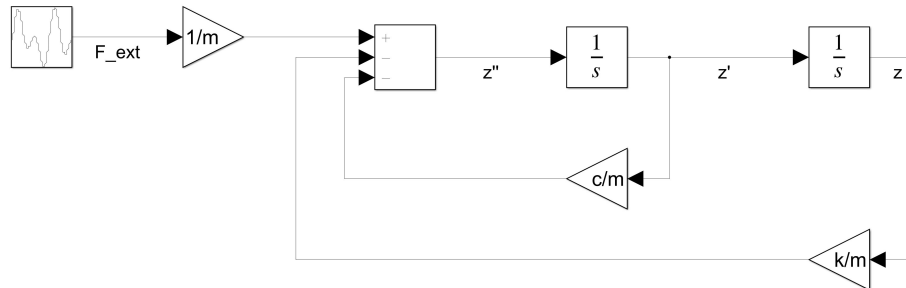


Figure 2: Simulink block diagram for linear mass-spring-dashpot model

2.2 Quadratic Damping

For a basic mass-spring-dashpot model, Assumption C allowed us to write a differential equation of motion that could be solved by hand. However, most dashpots consist of a plunger inside a fluid-filled piston, which can be modeled using a well-known result from fluid mechanics. This result is that the drag force, F_d , for a solid object in a laminar flow is

$$F_d = \frac{1}{2} C_D A \rho v^2$$

Here, ρ is the mass density of the fluid, A is the area normal to the fluid flow, v is the object's velocity, and C_D is the drag coefficient, which depends on the geometry of the object [1]. If we characterize the dashpot with this equation rather than $F_d = -c\dot{z}$, then **Equation 1** becomes

$$m\ddot{z} + q|\dot{z}|\dot{z} + kz = F_{ext}(t) \quad (2)$$

where $q = \frac{1}{2} C_D A \rho$ for more concise notation.² A Simulink block diagram for **Equation 2** is shown in **Figure 3**.

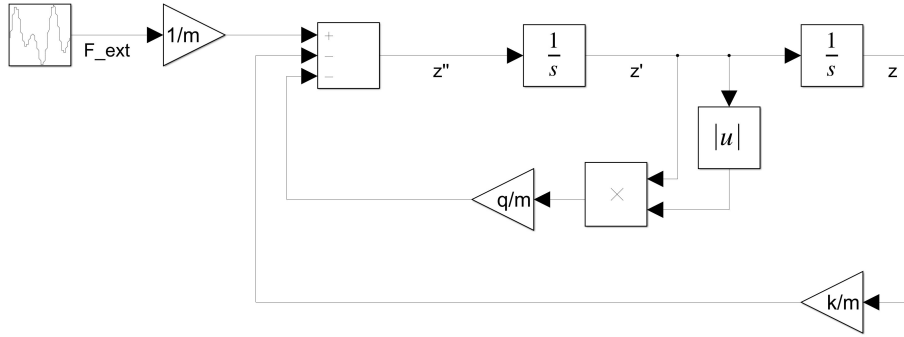


Figure 3: Simulink block diagram for mass-spring-dashpot model with quadratic damping

2.3 Quarter-Car Simulation

2.3.1 Choosing Forcing Function

Since **Equation 2** is nonlinear and piecewise defined, we choose to evaluate by simulation rather than by hand. This simulation allows us to compare a quadratically damped system to a linearly damped system.

In these simulations, we assume the damped oscillator is attached to a wheel which is on flat road until it enters a pothole. We aim to compare the responses of linear and quadratically damped systems to potholes.

²The damping term is written using $|\dot{z}|\dot{z}$ rather than \dot{z}^2 because the damping force will always oppose the velocity, and the sign of $-\dot{z}^2$ is negative no matter the sign of \dot{z} , whereas $-|\dot{z}|\dot{z}$ always has the opposite sign of \dot{z} .

Let there be an imposed height $h(t)$ on the wheel. The forcing function, is then

$$F_{ext}(t) = m\ddot{h}(t)$$

We now consider a proper function $h(t)$ to represent the displacement from a pothole. The most logical choice is a linear combination of delayed step functions:

$$h(t) = \begin{cases} 0 & t \leq t_1 \\ -d_p & t_1 < t \leq t_2 \\ 0 & t > t_2 \end{cases} \quad (3)$$

Here, d_p is the depth of the pothole and the wheel is only in the pothole for $t \in [t_1, t_2]$. However, F_{ext} is the second derivative of h , and would therefore be undefined at t_1 and t_2 . Therefore, we choose to instead approximate the piecewise function **Equation 3** by a continuous one. We choose to approximate step functions as logistic functions with very fast decay rates. Therefore, the pothole displacement is modeled as

$$h(t) = -d_p\sigma(t; t_1, \lambda) + d_p\sigma(t; t_2, \lambda) \quad (4)$$

where σ is the logistic function

$$\sigma(t; \tau, \lambda) = \frac{1}{1 + e^{-\lambda(t-\tau)}}$$

2.3.2 Choosing Parameter Values

For **Equation 4** to approximate **Equation 3** well, it is imperative that the time scale of action on the logistic curve is much smaller than the time the separation between t_1 and t_2 . In other words, $\frac{1}{\lambda} \ll t_2 - t_1$. This ensures that the "bottom" of the pothole is relatively flat by letting the time the wheel is in the pothole to be much larger than the time it takes for the wheel to fall into the pothole.

We must also choose values for t_1 and t_2 . Assuming the wheel has a constant velocity v and the pothole has width w_p , the amount of time the wheel is in the pothole is given by

$$t_2 - t_1 = \frac{w_p}{v}$$

Assuming that the velocity is 30 miles per hour, and the pothole width is 1 meter, we find $t_2 - t_1$ is 0.0746 seconds. We choose to let $\lambda = 500 \text{ s}^{-1}$ and d_p be 3 inches, which gives the forcing function shown in **Figure 4**.³

³While we could choose an arbitrarily large λ to get an even better approximation of a step function, it will make the derivative of the function increasingly hard to estimate for the simulation software, which has a nonzero time step. Therefore, we choose λ to be large enough to provide an acceptable step function approximation, though not so large that it introduces significant discretization error into the simulation.

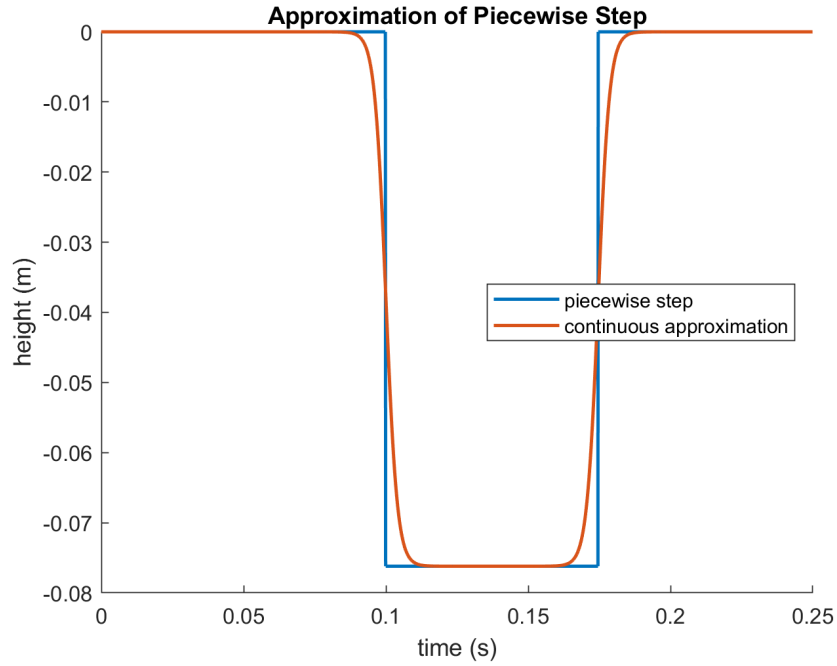


Figure 4: Step function desired and approximation actually used in simulation.

We also need numerical values for m , k , c , and q to run a simulation. We use the same values as Haris and Aboud's [3] quarter-car model for m , k , and c . The value of q was chosen such that the oscillations of the quadratically damped system were of similar amplitude to the linear system. The parameters used are shown in **Table 1**.

Parameter	Value	Units
k	1600	$\text{kN}\cdot\text{m}^{-1}$
c	1	$\text{kN}\cdot\text{s}\cdot\text{m}^{-1}$
m	280	kg
q	800	$\text{N}\cdot\text{s}^2\cdot\text{m}^{-2}$
v	13.4	m^{-1}
w_p	1	m
d_p	7.6	cm
λ	100	s^{-1}

Table 1: Top: car parameters used in quarter-car simulation. Bottom: forcing function parameters used in quarter-car simulation

2.3.3 Simulation Results

Using Simulink with a time step of $100 \mu\text{s}$, we examined the response of the linearly damped and quadratically damped systems to a pothole forcing function. The block diagrams are shown in **Figures 2 and 3**. The simulation results are shown in **Figure 5**.

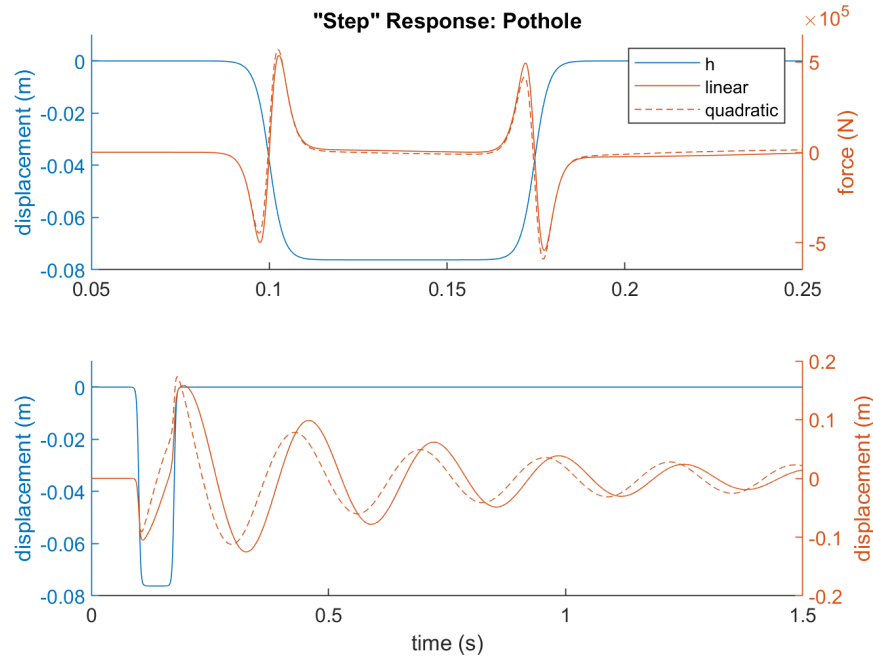


Figure 5: Top: force response near pothole. Bottom: displacement response to pothole

2.3.4 Simulation Analysis

The graph of force versus time shows mostly what we would expect. At the first falling edge, the force sharply moves downward, though after the wheel hits the bottom of the pothole, there is a large acceleration, upward. The rising edge is much the same, but with the signs reversed. The force graph seems to show zero force between the edges and after the falling edge, despite the fact that the displacement graph shows oscillation occurring these periods. This is because while there is a force at these times, it is very small compared to the force at the edges of the pothole, so it doesn't even show up on the graph.

The displacement graph shows much what we would expect as well: an initial displacement downward as the car enters the pothole followed by a positive displacement as the car rebounds upward, a sharp displacement upward followed at the rising edge followed by a displacement downward as the spring

recompresses, and then oscillation.

The position graph is where the difference between quadratic and linear damping becomes clear. In the first two local maxima following the pothole, it is clear that the linearly damped system is oscillating with higher amplitude. However, at the last local maximum, it is clear that the quadratically damped oscillator has a higher amplitude. This is exactly what we would expect; the quadratic damping is more resistant to motion at higher amplitudes but relaxes at lower amplitudes. So while the quadratic damper may reduce the amplitude of oscillation sharply initially, it will take much longer for its oscillations to die off than the oscillations from linear damper.

3 Half-Car Model

3.1 Model Background

The models considered in 2.1 and 2.2 only include a single mass-spring-damper, though cars' suspension systems actually consist of springs and dampers for each wheel. Considering all four wheels, the system becomes very complicated to model, since it will have three rotational degrees of freedom (see **Figure 6**). Therefore, we create a half-car model by modeling the front and rear axes as a single wheel. In this way, we consider pitch as the only form of rotation.

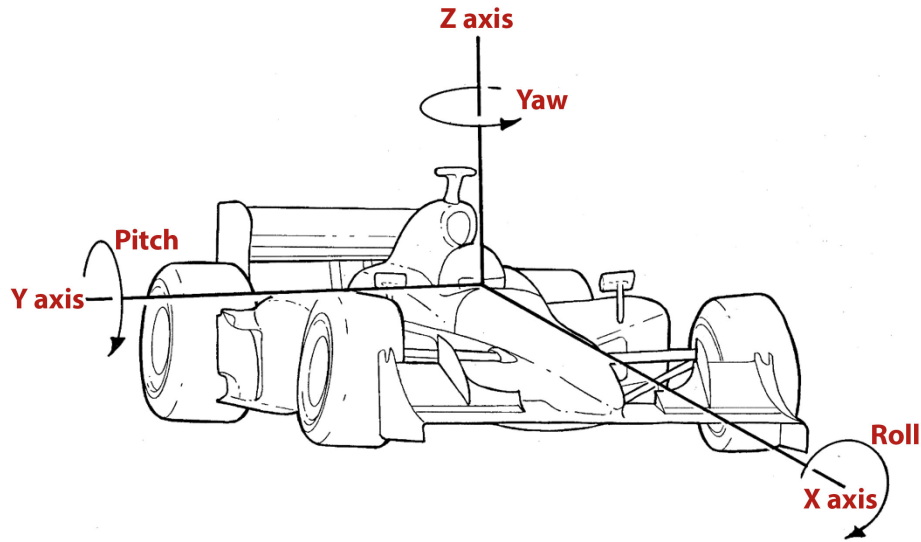


Figure 6: Rotational degrees of freedom for a car [6]

Initially, we form the half-car model by forming pin connections between the ends of a rigid body and two mass-spring-damper systems. We assume that the rigid body (the car chassis) has a moment of inertia I about its center of mass,

so that a force on one axle induces a torque in the rigid body, and therefore a force in the opposite direction on the other axle. Therefore, the suspension system behaves as a type of coupled oscillator.

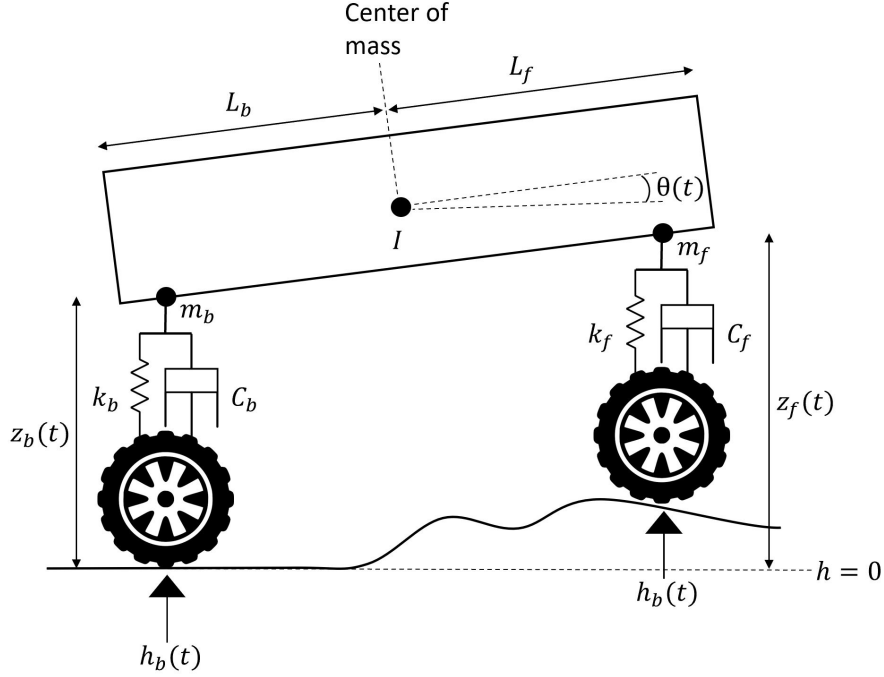


Figure 7: Coupled oscillator representation of half-car model

Notice that the state of the system in **Figure 7** is uniquely described by the three state variable (and their time derivatives): $z_f(t)$, $z_b(t)$, and $\theta(t)$. Notice also, that from basic trigonometry

$$\sin \theta = \frac{z_f - z_b}{L_f + L_b}$$

Since we can relate the state variables to each other in a way that involves no time derivatives, it means we need only two differential equations to model the system instead of three. Therefore, we will make a change of variables that will make the system less tedious to model: like Talukdar *et al.* [9], we will examine the vertical displacement of the center of mass, z_{cm} , rather than the vertical displacements of the two ends.

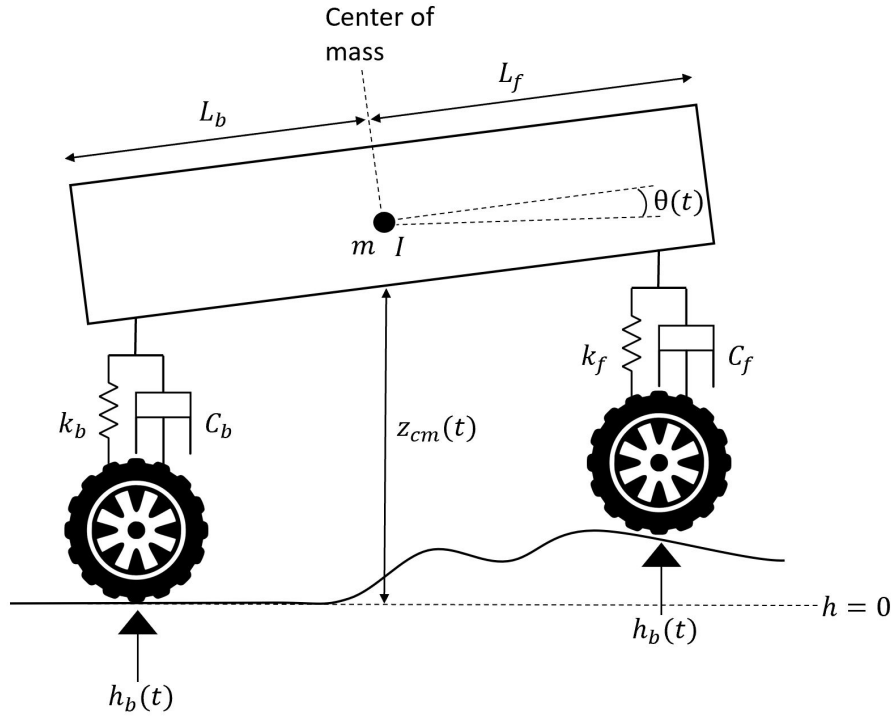


Figure 8: Half-car model schematic geometry after change of variables

3.2 Accounting for Rotation

As with the single mass-spring-damper, the equations of motion are derived from Newton's Second Law, which in this case is $\sum F = m\ddot{z}_{cm}$. We also utilize the rotational equivalent of Newton's Second Law which is $\sum N = I\ddot{\theta}$, where N is the first moment of force, commonly referred to as torque. Torques occur about points when a force F acts a distance r from the point. From trigonometry, the distance r from the center of mass to the line of action of the force from either of the spring-dashpot assemblies is given by

$$r = L \cos \theta$$

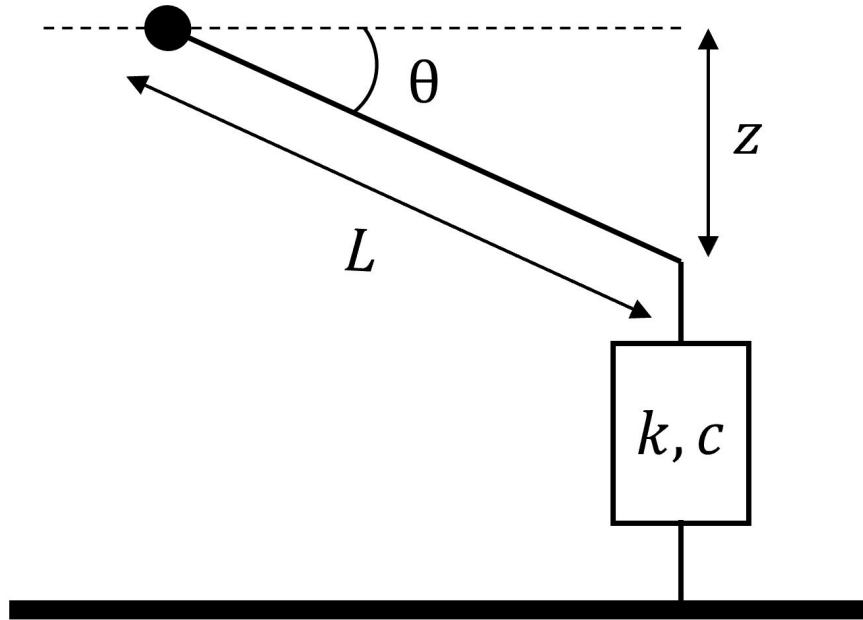


Figure 9: Relation between translational (z) and angular (θ) displacements

Notice also in **Figure 9** that $z = L \sin \theta$. Therefore, for rotational and translational motion, we can write four equations for springs/dashpots relating the displacements/velocities to accelerations. For springs:

$$F_s = -kz$$

$$F_s = -kL \cos \theta \sin \theta$$

$$N_s = -kLz$$

$$N_s = -kL^2 \cos \theta \sin \theta$$

and for dashpots

$$F_d = -k\dot{z}$$

$$F_d = -kL \cos \theta \sin \dot{\theta}$$

$$N_d = -kL\dot{z}$$

$$N_d = -kL^2 \cos \theta \sin \dot{\theta}$$

Since θ is a state variable, all expressions involving θ are nonlinear. However, if we assume small angles of displacement, we can approximate $\cos \theta \sin \theta$ by the first term in its power series expansion. Making the approximation $\cos \theta \sin \theta \approx \theta$, we are left with a linear system of differential equations. Including

the forces and torques from all components, we can write equations for the total force and torque as follows:

$$\begin{aligned}\sum F_{cm} = m\ddot{z}_{cm} &= -c_f(\dot{z}_{cm} - \dot{h}_f) - c_b(\dot{z}_{cm} - \dot{h}_b) - k_f(z_{cm} - h_f) - k_b(z_{cm} - h_b) \\ &\quad - (c_f L_f - c_b L_b)\dot{\theta} - (k_f L_f - k_b L_b)\theta \\ &= -(c_f + c_b)\dot{z}_{cm} - (k_f + k_b)z_{cm} - (c_f L_f - c_b L_b)\dot{\theta} - (k_f L_f - k_b L_b)\theta \\ &\quad + c_f \dot{h}_f + c_b \dot{h}_b + k_f h_f + k_b h_b\end{aligned}\tag{5}$$

$$\begin{aligned}\sum N_{cm} = I\ddot{\theta} &= -c_f L_f(\dot{z}_{cm} - \dot{h}_f) + c_b L_b(\dot{z}_{cm} - \dot{h}_b) - k_f L_f(z_{cm} - h_f) + k_b L_b(z_{cm} - h_f) \\ &\quad - (c_f L_f^2 + c_b L_b^2)\dot{\theta} - (k_f L_f^2 + k_b L_b^2)\theta \\ &= -(c_f L_f - c_b L_b)\dot{z}_{cm} - (k_f L_f - k_b L_b)z_{cm} - (c_f L_f^2 + c_b L_b^2)\dot{\theta} - (k_f L_f + c_b L_b)\theta \\ &\quad + c_f L_f \dot{h}_f - c_b L_b \dot{h}_b + k_f L_f h_f - k_b L_b h_b\end{aligned}\tag{6}$$

The first lines of **Equations 5 and 6** have terms arranged according to the force/torque exerted by each component. In the second line, they are rewritten so that terms are grouped according to state variables and their derivatives.

3.3 Half-Car Simulation

This system can be rewritten in a more concise matrix form that will allow for a simulation model to be built more easily:

$$\mathbf{M}\ddot{\mathbf{x}} + \mathbf{C}\dot{\mathbf{x}} + \mathbf{K}\mathbf{x} = \mathbf{A}\dot{\mathbf{h}} + \mathbf{B}\mathbf{h}\tag{7}$$

$$\begin{aligned}\mathbf{M} &= \begin{bmatrix} m & 0 \\ 0 & I \end{bmatrix}, \quad \mathbf{C} = \begin{bmatrix} c_f + c_b & c_f L_f - c_b L_b \\ c_f L_f - c_b L_b & c_f L_f^2 + c_b L_b^2 \end{bmatrix}, \quad \mathbf{K} = \begin{bmatrix} k_f + k_b & k_f L_f - k_b L_b \\ k_f L_f - k_b L_b & k_f L_f^2 + k_b L_b^2 \end{bmatrix} \\ \mathbf{x} &= \begin{bmatrix} z_{cm} \\ \theta \end{bmatrix}, \quad \mathbf{A} = \begin{bmatrix} c_f & c_b \\ c_f L_f & -c_b L_b \end{bmatrix}, \quad \mathbf{B} = \begin{bmatrix} k_f & k_b \\ k_f L_f & -k_b L_b \end{bmatrix}, \quad \mathbf{h} = \begin{bmatrix} h_f \\ h_b \end{bmatrix}\end{aligned}$$

We could transform the the system from a 2×2 second order system to a 4×4 first order system, which would allow us to use the State Space Form [7] to solve it by hand. This would allow us to find the transfer function and eigenvalues symbolically. However, we opt for a simpler approach: running numerical simulations given a single forcing function $\mathbf{h}(t)$ of interest. Just as in **2.3**, we examine the response to a pothole.

3.3.1 Choosing Forcing Function

For two wheels, we must now must consider the implications of a pothole for $h_f(t)$ and $h_b(t)$. Assuming constant velocity v , we can calculate a time delay, τ , between when the front wheel hits the pothole and when the back wheel hits the pothole based on the length of the car. The time delay is given by

$$\tau = \frac{L_f + L_b}{v}$$

The relation between the road heights in the front and back is then given by

$$h_b(t) = h_f(t - \tau)$$

3.3.2 Choosing Parameter Values

The half-car simulation requires a larger set of parameters than the quarter-car simulation. Since the half-car model accounts for rotational motion, we must have a numerical value for moment of inertia. We calculate the moment of inertia assuming the car is a thin rod of uniform density. The moment of inertia is then given by [8]:

$$I = \frac{1}{12}m(L_f + L_b)^2$$

By assuming symmetry of the system, i.e. $L_b = L_f$, $k_f = k_b$, $c_f = c_b$, we can use the parameter values used by Haris and Aboud [3] in their quarter-car model, and a length estimate [4]. For the half-car model, spring constants and damping coefficients must be multiplied by two, and mass must be multiplied by four, which gives:

Parameter	Value	Units
k	320	$\text{kN}\cdot\text{m}^{-1}$
c	2	$\text{kN}\cdot\text{s}\cdot\text{m}^{-1}$
m	1120	kg
$L_{1/2}$	2.3	m
I	1975	$\text{kg}\cdot\text{m}^2$
v	13.4	m^{-1}
w_p	1	m
d_p	7.6	cm
λ	100	s^{-1}

Table 2: Top: car parameters used in half-car simulation. Bottom: forcing function parameters used in half-car simulation

3.3.3 Simulation Results

The Simulink block diagram for the half-car model takes the following form:

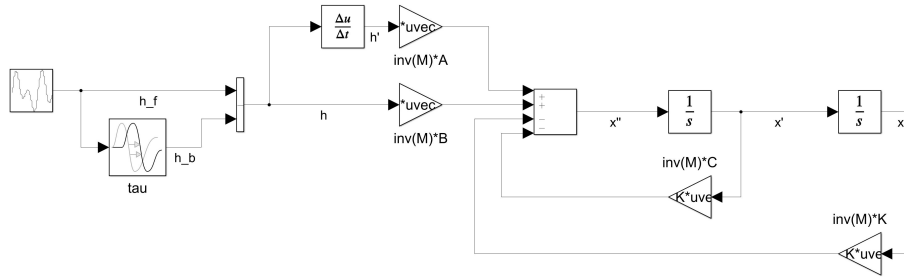


Figure 10: Simulink model used for half-car simulation

We ran the simulation for 1.5 seconds, with a fixed time step of $100 \mu\text{s}$. The results for force, translational displacement, torque, and angular displacements as functions of time are shown in **Figures 11 and 12**.

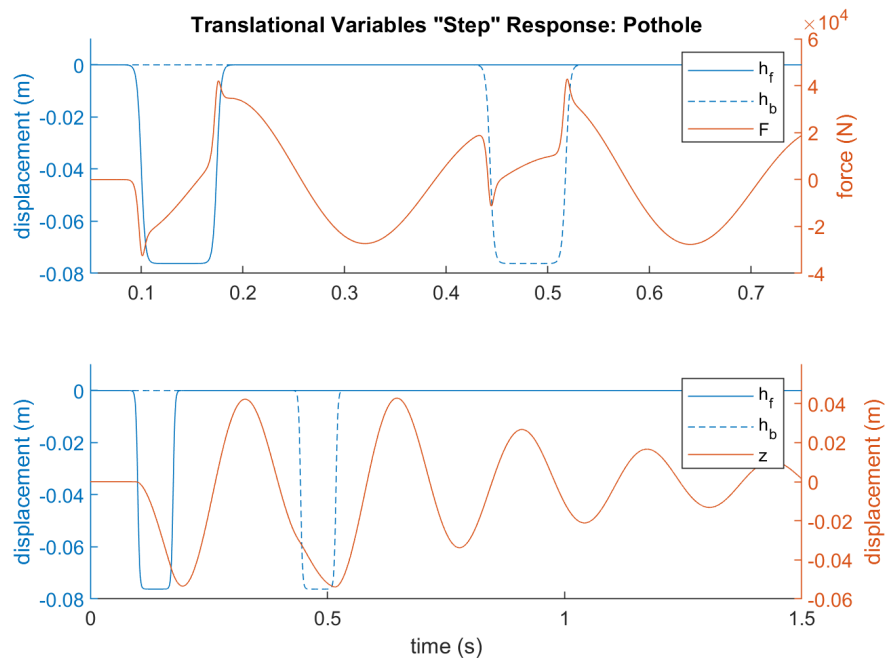


Figure 11: Half-car simulation results for translational variables

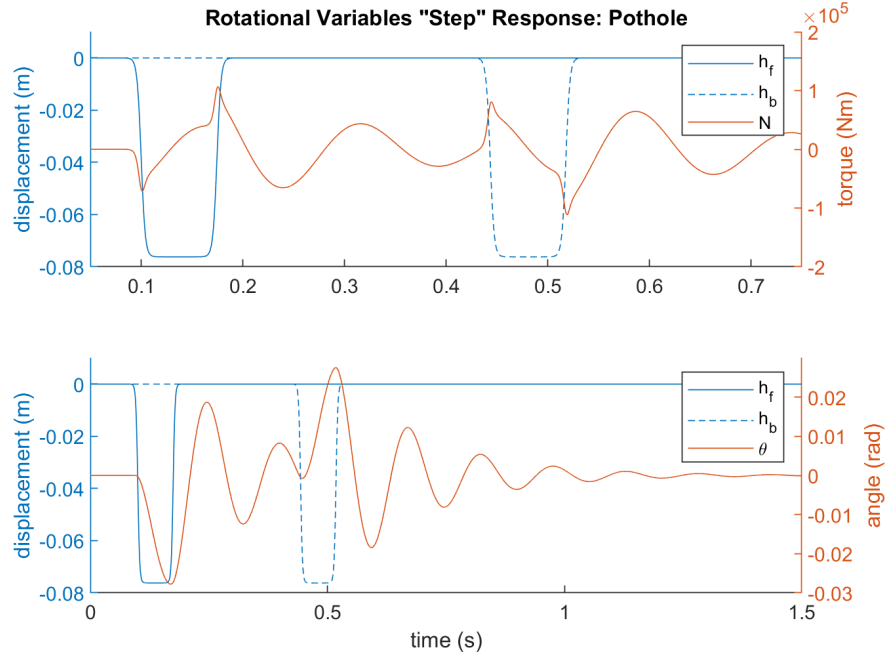


Figure 12: Half-car simulation results for rotational variables

3.3.4 Simulation Analysis

These simulations produce very interesting results. While we see large forces at the edges of the potholes, they are somewhat attenuated by the fact that only one wheel goes into the pothole at a time. This however means that the torques at the edges are quite large. After the car is out of the pothole, we see damped sinusoidal forces, displacements, torques and angles. It is interesting to see that the rotational motion happens much more quickly than the translation motion; the center of mass moves up and down at about 4 Hz while the car tilts back and forth at about 6 Hz. It is also interesting to notice that the rotational oscillation dies out much more quickly than the translational oscillation. While the rotational and translational motion are both governed by the same set of eigenvalues, it is likely that two eigenvectors of the form $\begin{bmatrix} a_1 \\ a_2 \end{bmatrix}$ and $\begin{bmatrix} b_1 \\ b_2 \end{bmatrix}$ satisfy $a_1 \gg a_2$ and $b_1 \ll b_2$. This would mean that solutions are possible where the behavior of z and θ are dominated by different eigenvalues.

4 Conclusion

In this work, we were able to compare the theoretical responses of a quarter-car suspensions made with linear and quadratic dampers. We found that the

quadratic damper reduced the maximum oscillation amplitude the system experienced, but that the oscillations persisted longer at an appreciable amplitude than they did for the linear damper.

We were also able to examine the theoretical translational and angular displacements of a half-car suspension. We found that for the pothole forcing function it was subjected to, the car experienced rotational oscillation at a higher frequency than vertical oscillation, but that the tilting motion died out more quickly than the bouncing motion.

This work makes significant strides, but leaves much follow up work open. The quadratic damper should continue to be investigated so its properties can be better understood. While there are no such things as transfer functions for nonlinear systems, a pseudo-transfer function at a specific forcing function amplitude could be derived to better understand the frequency response of the quadratically damped oscillator. Additionally, its step response produces oscillations that die out over time. The envelope function of these oscillations is unknown, and could be investigated by attempting to derive a closed form solution to the differential equation, or by fitting various curves to the local optima of the waveform. Additionally, it would be a worthwhile endeavor to replace the linear dampers in the half-car model with quadratic dampers to examine how the quadratic damping affects coupled oscillation.

References

- [1] [https://phys.libretexts.org/Bookshelves/Classical_Mechanics/Classical_Mechanics_\(Dourmashkin\)/08%3A_Applications_of_Newtons_Second_Law/8.06%3A_Drag_Forces_in_Fluids](https://phys.libretexts.org/Bookshelves/Classical_Mechanics/Classical_Mechanics_(Dourmashkin)/08%3A_Applications_of_Newtons_Second_Law/8.06%3A_Drag_Forces_in_Fluids)
- [2] <https://www.mathworks.com/help/simulink/slref/automotive-suspension.html>
- [3] https://www.researchgate.net/publication/328875576_Design_of_two_optimal_controllers_for_mechatronic_suspension_system
- [4] <https://mechanicbase.com/cars/average-car-length/#:~:text=of%20a%20Car%3F-,What%20is%20the%20Average%20Car%20Length%3F,of%20any%20car%20model's%20length.>
- [5] https://www.researchgate.net/figure/Drag-force-versus-velocity-in-the-surge-direction_fig36_230686999
- [6] <https://www.racecar-engineering.com/tech-explained/racecar-vehicle-dynamics-explained/attachment/racecar-vehicle-dynamics-roll-pitch-yaw/>
- [7] <https://lpsa.swarthmore.edu/Representations/SysRepSS.html>
- [8] https://en.wikipedia.org/wiki/List_of_moments_of_inertia
- [9] <https://ijret.org/volumes/2013v02/i10/IJRET20130210002.pdf>